Environmental Science & Technology

pubs.acs.org/est

Article

What Is the Molecular Weight of "High" Molecular Weight Dissolved Organic Matter?

Benjamin N. Granzow* and Daniel J. Repeta*

Cite This: *Environ. Sci. Technol.* 2024, 58, 14709−14717

Read Online

ACCESS | Metrics & More | Article Recommendations | Supporting Information

ABSTRACT: The use of ultrafiltration to isolate high molecular weight dissolved organic matter (HMWDOM) from seawater is a fundamental tool in the environmental organic chemist's toolbox. Yet, important characteristics of HMWDOM relevant to its origin and cycling, such as its molecular weight distribution, remain poorly defined. We used diffusion-ordered NMR spectroscopy coupled with mixed-mode chromatography to separate and characterize two major components of marine HMWDOM: acylpolysaccharides (APS) and high molecular weight humic substances (HS). The molecular weights (MWs) of APS and HS both fell within distinct, narrow envelopes; 2.0−16 kDa for APS and 0.9−6.5 kDa for HS. In water samples from the North Pacific Ocean the average MW of both components decreased with depth through the mesopelagic. However, the minimum MW of APS was >2 kDa, well above the molecular weight cutoff of the ultrafilter, suggesting APS removal processes below 2 kDa are highly efficient. The MW distribution of APS shows only small variations with depth, while the MW distribution of HS narrowed due to removal of HMW components. Despite the narrowing of the MW distribution, the concentration of HS did not decrease with depth between 15 and 915 m. This suggests that HMW HS produced in surface waters was either degraded into lower MW compounds without significant remineralization, or that HMW HS was remineralized but replaced by an additional source of HS in the mesopelagic ocean. Based on these results, we propose potential pathways for the production and removal of these major components of HMWDOM.

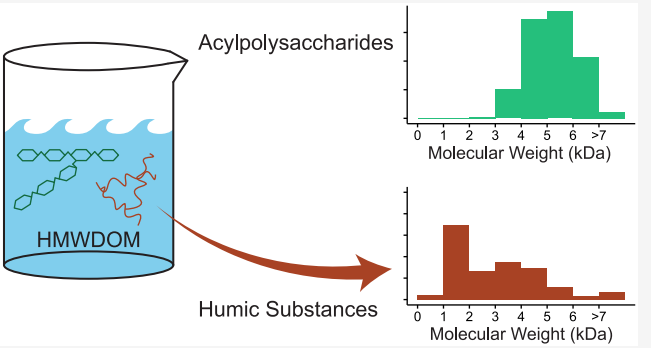

KEYWORDS: *High molecular weight dissolved organic matter, diffusion−ordered spectroscopy, humic substances, acylpolysaccharides*

INTRODUCTION

In natural waters, organic matter not retained by a 0.1−1 μm filter is operationally classified as "dissolved".[1−3] Dissolved organic matter (DOM) can be further separated into high molecular weight and low molecular weight fractions (HMWDOM and LMWDOM, respectively) by ultrafiltration (UF).[4−7] HMWDOM is nominally defined as having a molecular weight (MW) greater than the molecular weight cutoff (MWCO) of the ultrafilter (typically 1 kDa), and can account for up to a third of marine DOM and as much as two-thirds of DOM in freshwater systems.[8−19] The range of MWs included in this fraction is very broad, spanning several orders of magnitude. For example, Santschi et al.[20] found that a fraction of marine HMWDOM consisted of colloidal fibrils with an estimated MW approaching 1 MDa, while Hertkorn et al.[21] found that a humic-like component of HMWDOM primarily contained compounds with a MW range of 300−600 Da. In between these two extremes, biopolymers such as proteins and nucleic acids, have MWs between 10 to >70 kDa.[22−24]

The MW of biopolymers impacts their trace metal binding characteristics, their potential for aggregation and particle formation, and perhaps most importantly, their rate of degradation by heterotrophic bacteria and fungi.[25−28] To be assimilated, substrates need to be transported into cells through porin channels. These channels have MW restrictions of ≤800 Da. HMWDOM biopolymers >800 Da need to be hydrolyzed by extracellular or cell surface enzymes before being transported into the cell.[29−41] Up to 90% of the identifiable biopolymers in marine HMWDOM belong to a family of compositionally related acylpolysaccharides (APS) characterized by the high percentage of N-acetyl aminosugars that make up the polymer. The MW of APS will dictate the amount of extracellular hydrolysis needed before the cell can take them up.[15,42−44] Larger polysaccharides will require more hydrolysis steps to reach the ∼800 Da porin weight restriction. Models of APS lability propose that extracellular hydrolysis

Received: April 24, 2024
Revised: July 17, 2024
Accepted: July 18, 2024
Published: August 5, 2024

https://doi.org/10.1021/acs.est.4c03372
Environ. Sci. Technol. 2024, 58, 14709−14717

occurs slowly and is the rate-limiting step in APS degradation.[45] To better understand how MW controls the uptake rate of APS by heterotrophic bacteria and fungi, a refined description of the APS MW distribution is necessary.

Humic substances (HS), another major component of HMWDOM, comprise a broad class of compounds characterized as being carboxylic-rich and alicyclic.[21] Analysis of HS in HMWDOM by high-resolution mass spectrometry found that the intensity-weighted average MW of ions was 450 Da, much lower than the 1 kDa MWCO of the UF membranes used to collect the samples, and similar to the MW of HS extracted from seawater onto hydrophobic resins via solid-phase extraction (SPE).[21,46,47] The presence of LMW humic substances in the HMWDOM fraction could be due to a bias in the mass spectrometric analysis favoring the detection of LMW compounds or due to the inadvertent retention of LMW HS by the UF membrane due to fouling.[48−52] Measuring the MW distribution of HS will allow us to determine if there is a high molecular weight fraction of HS, or if LMW humic substances in HMWDOM are a result of membrane fouling or biases in mass spectrometric analyses.

In this study, the MW distributions of the APS and HS components in HMWDOM were measured by diffusion-order spectroscopy (DOSY).[53] DOSY is a pseudo-2D nuclear magnetic resonance (NMR) technique that measures the diffusion coefficient associated with signals in a one-dimensional (1D) ^{1}H spectrum. Using model compounds with a range of known MWs, a relationship between diffusivity and MW was developed. We used mixed-mode chromatography (MMC) to separate HMWDOM into fractions of different average MWs, improving the resolution of the DOSY technique and providing quantitative information about the amount of carbon in different MW fractions. By leveraging the strengths of MMC and DOSY, we characterized the MW distributions of APS and HS and proposed potential processes responsible for the transformation and degradation of these two major components of HMWDOM.

MATERIALS AND METHODS

Isolation and Concentration of DOM. Seawater samples were collected from 15, 628, and 915 m at the Natural Energy Laboratory Hawaii Authority (19° 43.66′ N, 156° 3.60′ W) in Kona, Hawaii (Figure S1 Supporting Information) during March 2019. HMWDOM was concentrated from filtered seawater (0.2 μm) by UF using a custom continuous UF system. For a complete description of the system see Repeta and Aluwihare,[54] but, in brief, filtered seawater was pumped through spiral wound UF membranes (GE-osmonics; GE Series) with a nominal MWCO of 1 kDa. Filtration was performed in 24-h batches and the HMWDOM concentrates (retentates) were reduced to ∼20 L, filtered through a 0.1 μm PES capsule filter, and frozen to await further processing.[55] This final concentrate contained the HMWDOM from approximately 10,000 L of seawater. After thawing, the sample concentrate was 0.2 μm filtered, reduced in volume to ∼2 L, and desalted by serial (×10) diafiltration with deionized water (2 L each). The desalted samples were lyophilized, yielding a fluffy, white powder (28−34% C). Approximately 15% of the total DOC in the original sample was recovered, giving similar yields as has been reported previsously.[56,57]

Mixed-Mode Chromatography of HMWDOM. Mixed mode chromatography (MMC) was used to separate constituents of HMWDOM into 11 fractions with decreasing molecular weight. MMC was performed with a column (7.8 × 300 mm, 9 μm; Supelcogel; Vo = 3.1 mL) packed with sulfonated (8% cross-linked) polystyrene/divinylbenzene gel with calcium as the counterion maintained at 45 °C on an Agilent HPLC (Agilent 1260 Series). MMC separates analytes primarily on the basis of their molecular weight, although a degree of separation also occurs due to selective interactions between polyhydroxyl moieties and the complexing (Ca^{2+}) cations on the column media.[58−60] Ultrapure water (18.2 MΩ) was used as the mobile phase at a flow rate of 0.25 mL min^{-1} and each analysis lasted for 40 min. One-minute fractions were collected between 17 and 28 min, coinciding with sample elution. Corresponding fractions from multiple collections were pooled. In total 243 chromatographic separations were performed for each sample depth. MMC recoveries were 94% C for the 15 m sample and 89% C for the 915 m sample. The missing carbon was lost during processing, either due to irreversible adsorption onto the column or during the subsequent transfer and drying steps.

Each of the 11 fractions was dried under vacuum at ambient temperature and dry weights were measured gravimetrically on a Sartorius Pro 11 balance. Subsamples from each fraction were submitted to the University of Hawaii at Mānoa SOEST Laboratory for Analytical Biogeochemistry for C and H content analysis, which was performed on an Exeter Analytical CE 440 Elemental Analyzer. A full description of the analytical protocol has been described previously.[61]

NMR Analysis of HMWDOM. NMR spectra were acquired on a Bruker Avance Neo NMR spectrometer operating at 400.13 MHz (B_0 = 9.4 T) using TopSpin 4.1.3 software. Samples were dissolved in 0.7 mL of D_2O (≥99.96 atom % D) to a final concentration of 1 mg mL^{-1}. All spectra were acquired on a Bruker Prodigy inverse geometry 5 mm z-gradient broad band probe. All spectra were acquired at 302 K. ^{1}H NMR spectra were acquired using a NOESY pulse program with presaturation water suppression (NOESYGPPR1D; Bruker). The 90° hard pulse length was set to 12 μs and a 10 ms mixing time was used. Acquisition time was 1.7 s and the relaxation delay (D1) was 2 s. For each spectrum, 128 scans were collected. Spectral subtraction was used to calculate the concentration of the components of APS and HS in each sample based on NMR peak area.[21] A full description of this calculation is in the Supporting Information.

DOSY experiments were performed using the STEBPGP1S19 pulse program (Bruker), which uses bipolar gradient pulses for diffusion, contains a z-axis spoiler gradient and uses a 3−9−19 water suppression sequence to reduce signal from the solvent peak. The maximum gradient strength was 53.5 G cm^{-1} and 32 linear gradient steps were used with power increments from 2 to 95% of the maximum gradient strength. For each gradient increment, 256 scans were collected. Gradient recovery delay was 200 μs, relaxation delay (D1) was 2 s, and the diffusion time (Δ) was 0.2 s. The magnetic field gradient pulse length ($\delta/2$) was 1150 μs. DOSY spectra were processed with Bruker Dynamic Center 2.7.1 and diffusion coefficients were calculated using a monoexponential fit. A Bayesian method from MestReNova 14.2.3[62] and the multiexponential fit (two exponentials) DOSY utility from the General NMR Analysis Toolbox 1.3.2[63] were also used and yielded the same diffusivity values. All signals above baseline were analyzed. The full parameter set for the DOSY experiment can be found in the Supporting Information.

https://doi.org/10.1021/acs.est.4c03372
Environ. Sci. Technol. 2024, 58, 14709−14717

Three classes of MW standards were used to precalibrate DOSY experiments and to create a MW−diffusivity standard curve (Figure S2, Supporting Information). Polystyrenesulfonate, globular protein, and pullulan standards (all from PSS Polymer Standard Services, Germany) with a MW range of 0.3 to 22 kDa were used to represent the continuum of expected MWs and conformations in HMWDOM. Suwannee River Humic Acid (International Humic Substances Society) was also analyzed. The MW distribution of Suwannee River Humic Acid has been extensively studied making it an excellent natural organic matter standard for intercomparison.[64−68] Validation of the DOSY technique for estimating DOM MW is discussed in the Supporting Information (Table S1). To confirm that freeze-drying did not significantly shift the MW of the samples, aliquots of the HMWDOM retentate were analyzed before and after lyophilization. We found no measurable effect of freeze-drying on the ^{1}H NMR spectrum or on measurements of diffusion coefficient.

RESULTS AND DISCUSSION

Proton NMR Spectroscopy of HMWDOM. ^{1}H NMR spectra of HMWDOM (Figure 1) are similar to those

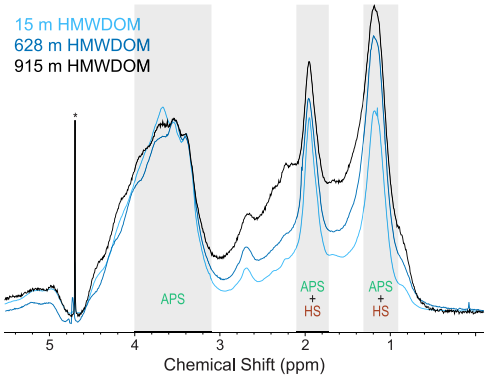

Figure 1. ^{1}H NMR spectra of 15 m (light blue), 628 m (dark blue), and 915 m (black) HMWDOM in D_2O. All spectra were normalized to signal intensity at 3.3 ppm. Shaded regions (4.0−3.1 ppm; 2.1−1.7 ppm; and 1.3−0.9 ppm) indicate portions of the spectra that have significant APS signal. The intensities of the broad HS signals (4−1 ppm) increase with depth, indicating a greater contribution of HS in the deeper HMWDOM samples. The chemical shifts are referenced to the water peak at 4.70 ppm (*).

previously reported for marine and freshwater samples.[43,69,70] There is a broad peak centered at 3.5 ppm from HC-OD protons assigned to carbohydrates and peaks at 2.0 and 1.2 ppm from *N*-acetyl functional groups and alkyl moieties, respectively. The peak at 3.5 ppm is associated primarily with APS, while the peaks at 2.0 and 1.2 ppm are the combination of signals from N-acetyl and 6-deoxy sugars in APS, and alkyl groups in HS. The large variety of alkyl groups found in HS leads to a broadening of the 1.2 ppm peak in samples with a large HS component. Beneath these signals, there is a broad signal between 3.1 and 0.8 ppm associated with alicyclic and aliphatic protons found in HS.[21,43] The relative peak areas of the APS and HS signals provide an estimate for the amount of each component present in the sample. The HS signal becomes more pronounced in the deeper samples (Figure 1, black), indicating that the proportion of HS in HMWDOM increases with depth.

Molecular Weight of APS and HS in HMWDOM. The MW of the APS component of the 15, 628, and 915 m HMWDOM were found to be 6.1 ± 0.8, 4.4 ± 0.2, and 3.1 ± 0.3 kDa while the HS MWs were 2.7 ± 0.6, 1.6 ± 0.2, and 1.3 ± 0.2 kDa, respectively. The reported uncertainties combine the error in diffusivity curve fitting based on covariance analysis with the error of the standard curve linear regression. Uncertainties are not a measure of the MW distribution of each component but instead indicate the precision of the MW measurement using DOSY−derived diffusivities.[71] These results suggest that prior estimates of the average MW of HMWDOM were accurate; the MW of most of the HMWDOM falls between 1 and 10 kDa.[72−75]

Diffusivities derived via the DOSY technique are weighted average values. DOSY measures the decrease in signal intensity at a given chemical shift due to diffusion. If two (or more) components have signals at the same chemical shift and similar diffusion coefficients, the diffusivity measured by DOSY will represent the weighted average of the decreases in signal intensity of the those components. To determine the MW of APS and HS in HMWDOM, the values of their respective diffusion coefficients were determined via DOSY and were assigned from regions of the ^{1}H NMR spectra where the signal can be attributed largely to a single component (3.38 and 2.20 ppm for APS and HS, respectively). The diffusivity values at other chemical shifts (for example 1.2 and 2.0 ppm) are weighted averages of the MWs of HS and APS constituents, and their diffusivity values therefore reflect the relative contributions from each constituent. This effect causes the DOSY signal to shift in the diffusion dimension (*Y*-axis) between two extrema that represent the diffusion coefficients of the two components (Figure 2A). The diffusivity at 1.2 ppm, for example, is greater than the diffusivity at 3.38 ppm where the APS signal dominates, but smaller than the diffusivity at 2.20 ppm where the HS signal dominates. Importantly, the APS MW assignment represents a lower bound as there is likely some contribution from HS in the signal at 3.38 ppm. Likewise, the HS MW assignment represents an upper bound as there is likely some signal contribution from APS.

Trends in MW of HMWDOM with Depth. The DOSY analyses showed that the average diffusivity of HMWDOM increases with depth, indicating that there is a decrease in the average MW of HMWDOM between 15 and 915 m (Figure 2B). Many processes such as exoenzyme catabolism of APS and ultraviolet (UV) degradation of HS have been proposed for the breakdown of HMWDOM, resulting in the production of lower molecular weight compounds.[76−78] As the measured MW is a weighted average, it is unclear whether higher MW components within HMWDOM were preferentially removed, leaving only the lower MW components behind, or if all components within HMWDOM underwent a decrease in MW with depth. These two scenarios can be distinguished by comparing the molecular weight distribution of APS and HS between samples. The molecular weight distribution represents the range and relative proportion of the different components within a sample. For example, if most APS constituents all fall within a narrow MW envelope, the range in diffusivity measured at 3.38 ppm will be small. Conversely, if APS constituents are evenly distributed across a wide range of MWs, the range in diffusivity at 3.38 ppm will be broad (Figure S3, Supporting Information). The preferential removal of higher MW APS should decrease the range or broadness of the

https://doi.org/10.1021/acs.est.4c03372
Environ. Sci. Technol. 2024, 58, 14709−14717

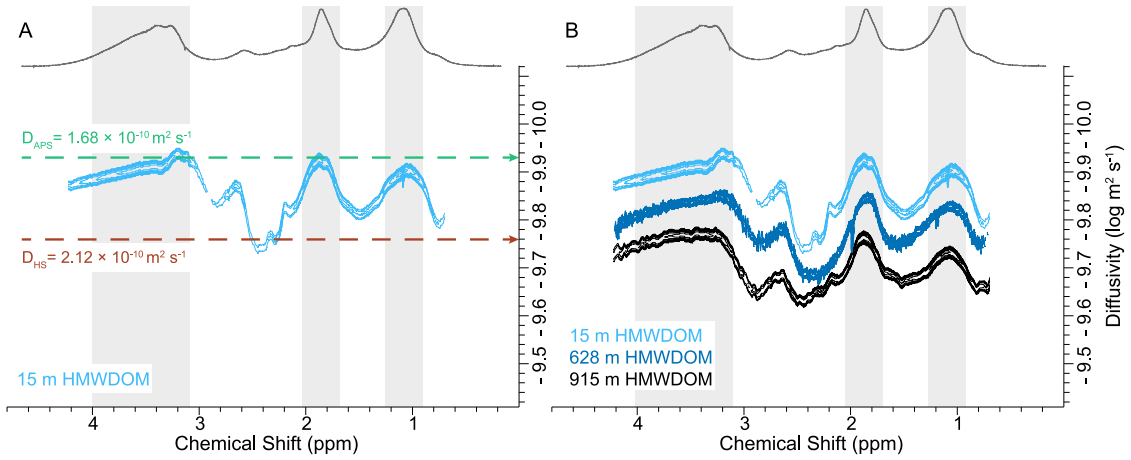

Figure 2. Diffusivity−chemical shift contour plots of the DOSY spectra of HMWDOM samples. Diffusivity is plotted on the vertical axis. A smaller (more negative) diffusivity corresponds to a higher MW. The 1D spectrum (gray trace) atop the plots is a projection of the 15 m sample DOSY spectrum. (A) The 15 m HMWDOM DOSY spectrum displays diffusivity signals which can be attributed to APS (shaded regions; 4.0−3.1; 2.1−1.7; and 1.3−0.9 ppm) and HS (3.1−2.1; 1.7−1.3 ppm). The diffusivity of the APS component (1.68 × 10^{-10} m^2 s^{-1}; green dashed arrow) is smaller than the diffusivity of the HS component (2.12 × 10^{-10} m^2 s^{-1}; red dashed arrow) indicating that the APS has a higher MW than the HS. (B) The DOSY spectra for HMWDOM collected at three depths show that the diffusivity increases with depth, signifying that the MW of HMWDOM decreases with depth. The chemical shifts are referenced to the water peak at 4.70 ppm (not shown).

MW distribution, resulting in a change in the diffusivity spectra at 3.38 ppm. In contrast, if all components within APS decreased in MW with depth we would expect little change in the broadness of the MW distribution, despite a decrease in the average MW.

To quantitatively compare the MW distribution for APS and HS, the span factor was computed. Span provides a unitless metric for the broadness of the MW distribution; components with a broader range of MWs will have higher span values, while components with a narrow MW distribution will have low span values. To determine the span factor, the tenth, fiftieth, and ninetieth percentiles (D_{v10}, D_{v50}, and D_{v90} respectively) of the MW distribution were calculated and span was computed as $(D_{v90} - D_{v10})/D_{v50}$ (Figure S3, Supporting Information). The APS spans in the 15, 628, and 915 m samples were 0.19, 0.15, and 0.15, respectively. The APS span decreased only slightly between the surface and the deep samples. In contrast, the corresponding spans for HS were 0.54, 0.45, and 0.28. The span of the HS MW distribution in the 915 m sample was considerably narrower than the MW distribution of the 15 m sample. The MW distribution of HS in the 628 m sample displayed an intermediate span between surface and deep HS. While the small decrease in the APS MW span suggests some preferential removal of HMW material, the large decrease in MW between 15 and 915 m suggests that the entire APS fraction decreased in MW with depth. The decrease in the HS span with depth on the other hand, suggests that higher MW HS were preferentially removed, resulting in a decrease in both MW and span with depth.

Distribution of Carbon within the MW Envelope of HMWDOM. To further describe the MW distribution of HS and APS, MMC was used to separate these HMWDOM components by MW. The amount of carbon recovered in each fraction of the MMC is shown in Figure 3. Only HMWDOM from 15 and 915 m were analyzed as the ^{1}H and DOSY NMR spectra suggest a smooth transition in MW with depth ($MW_{15m} > MW_{628m} > MW_{915m}$). For both samples, most of the carbon eluted between Ve/Vo = 1.5−1.9 (F3−F8), although a relatively greater amount of material eluted in the later

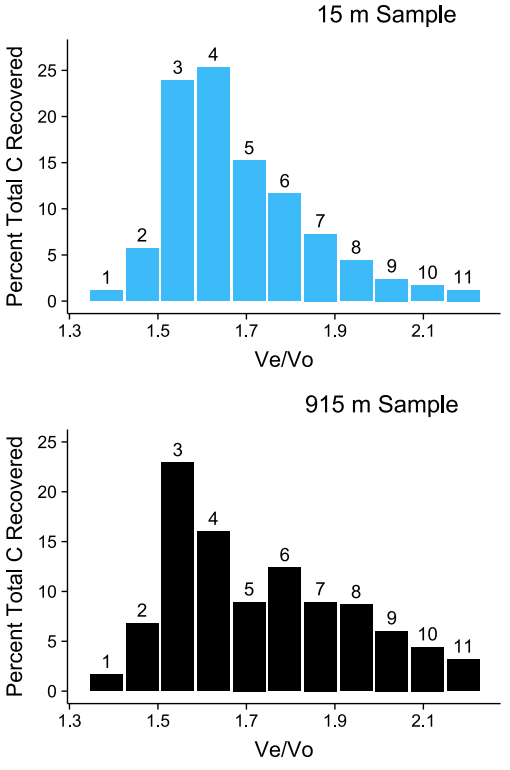

Figure 3. Relative amount of carbon recovered in each MMC fraction of the 15 m (light blue) and the 915 m (black) HMWDOM samples. Ve/Vo signifies the ratio of the elution volume to the void volume of the column. The fraction numbers are given above the bars. More than 60% of the material eluted in the middle of the chromatographic run (F3−F6, Ve/Vo = 1.5−1.8).

fractions (F7−F11, Ve/Vo = 1.9−2.2) of the 915 m sample compared to the 15 m sample, indicating a greater proportion of 915 m HMWDOM was low MW. These results are consistent with the NMR data that suggest HS comprises a larger fraction of the 915 m sample.

https://doi.org/10.1021/acs.est.4c03372
Environ. Sci. Technol. 2024, 58, 14709−14717

NMR Analysis of HMWDOM MMC Fractions. ^{1}H NMR spectra of the MMC fractions (Figure 4) show a change in

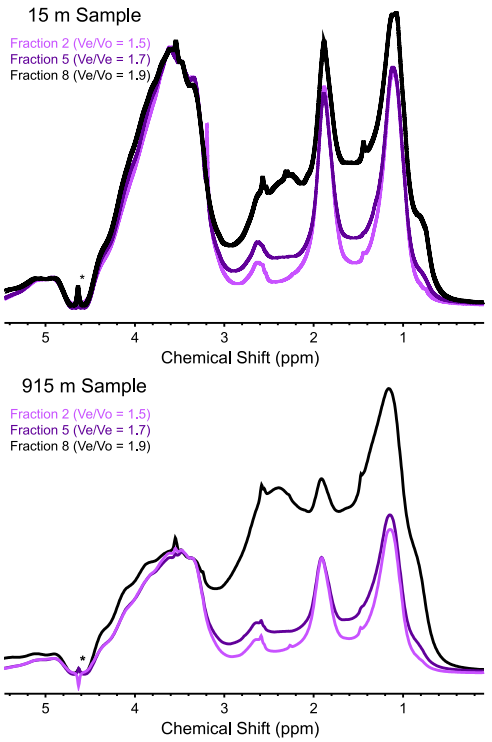

Figure 4. ^{1}H NMR spectra of select MMC fractions. Fraction 2 (18−19 min, light purple), Fraction 5 (21−22 min, dark purple), and Fraction 8 (24−25 min, black), illustrate the compositional changes that occur throughout the chromatography. Spectral intensities are normalized at 3.3 ppm. Peaks at 3.5 (**H**C-OD) and 2.0 (*N*-acetyl) ppm are attributed to APS while the broad signals at 2.2 and 1.5 ppm are attributed to HS. The peak at 1.2 ppm includes contributions from both APS (C**H**$_3$ in 6-deoxy-sugars) and HS. The chemical shifts are referenced to the water peak at 4.70 ppm (*).

sample composition across the MMC separation. The peaks attributed primarily to APS (3.3 and 1.8 ppm) decrease in relative intensity in the later eluting fractions, while the regions associated with HS (2.2 and 1.2 ppm) increase. Fractions with greater elution volumes have a larger proportion of HS relative to APS. The peak at 1.2 ppm includes contributions from both HS and APS. In the later-eluting fractions, the 1.2 ppm peak increases in relative intensity and peak width measured at half height due to the increased relative contribution of HS to this peak.

DOSY analysis of the MMC fractions from the 15 and 915 m samples shows that both APS and HS in earlier-eluting fractions have higher MWs than later-eluting fractions (Figure 5). MWs of the two components in each fraction are plotted in Figure 6. The MW of both components plateau in the later-eluting fractions (F8−F11) of each sample, with the APS reaching a minimum MW of 3.5 and 2.0 kDa in the 15 and 915 m samples respectively, and the HS reaching a minimum MW of 0.9 kDa at both depths. Most of the HMWDOM sample is above the nominal 1 kDa MWCO of the filter, suggesting that little membrane fouling and retention of LMW HS occurred. The DOSY results confirm that both MW and composition shift across the MMC separation. The MW of HMWDOM is controlled, in part, by the distribution of the chemical components, and discussions of processes such as

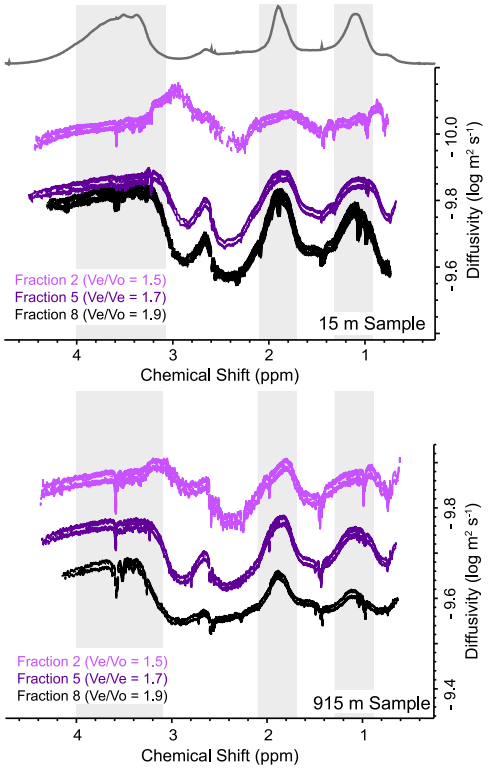

Figure 5. DOSY spectra of MMC fractions 2 (18−19 min, light purple), 5 (21−22 min, dark purple), and 8 (24−25 min, black), from 15 and 915 m HMWDOM. Diffusivity is plotted on the vertical axis. A lower diffusivity corresponds to a higher MW. MW was calculated from the diffusivity values measured at 3.38 and 2.20 ppm for the APS (shaded regions) and HS components, respectively. The chemical shifts are referenced to the water peak at 4.70 ppm (not shown).

bacterial and fungal degradation of DOM, or characterizations of DOM lability that use MW as a metric, must also consider the chemical makeup of the sample rather than treating HMWDOM as a monolithic substance.

APS and HS as Two Major Components of HMWDOM. HMWDOM has two major components: APS and HS.[69] Each component has a different MW distribution. The sums of the mass-weighted average of MWs of the MMC fractions for APS (6.1 ± 2.0 and 3.2 ± 1.0 kDa for the 15 and 915 m samples, respectively) were very similar to the average MW measured for APS in the whole HMWDOM samples (6.1 ± 0.8 and 3.1 ± 0.3 for the 15 and 915 m samples). Similarly, the average MW of MMC fractions for HS (1.8 ± 1.3 and 1.1 ± 0.4 kDa for the 15 and 915 m samples, respectively) were similar to the MWs measured for HS in whole HMWDOM (2.7 ± 0.6 and 1.3 ± 0.2 kDa for the 15 and 915 m samples). Figure 7 shows a histogram of total carbon vs MW for APS and HS in each sample. From the MW distributions in these two samples, we discuss possible pathways through which APS and HS are degraded.

The APS from the 15 m sample had an average MW of 6.1 ± 0.8 kDa, and an average degree of polymerization (DP) of 35 sugars, assuming a monosaccharide content of ∼50% *N*-acetyl sugars.[69,79,80] At 915 m, the APS MW decreased to 3.1 ± 0.3 kDa, equivalent to DP−18. Previous studies of APS found that the relative abundance of major neutral sugars did not shift substantially with depth, suggesting the polysaccharide from each depth has a similar composition.[43,54] The MW of APS decreases with depth, and the MW distribution at each depth

https://doi.org/10.1021/acs.est.4c03372
Environ. Sci. Technol. 2024, 58, 14709−14717

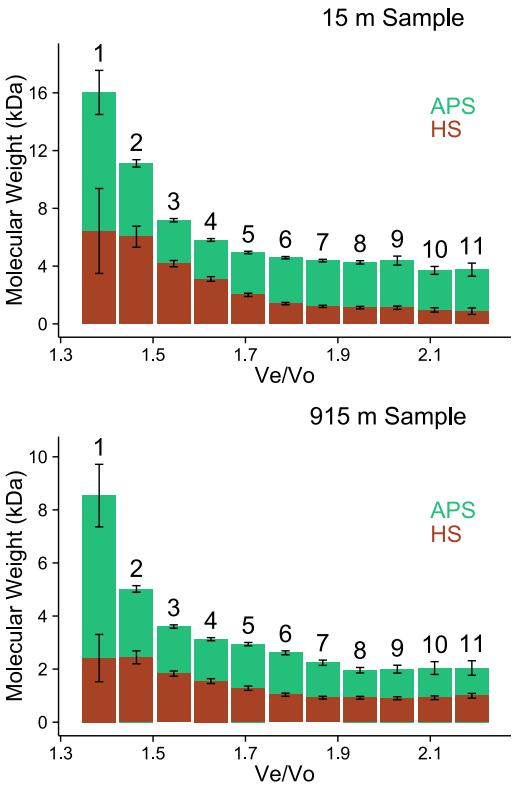

Figure 6. Average MW of HMWDOM APS (green) and HS (red) in MMC fractions for the 15 and 915 m samples. Ve/Vo signifies the ratio of the elution volume to the void volume of the column. Error bars represent the uncertainty associated with the MW computation and do not represent the MW range of each component. APS MW was calculated using a pullulan standard curve, and HS MW was calculated using a polystyrenesulfonate standard curve. The numbers above the columns denote the collected fraction number. APS has a higher MW than HS in all fractions, and both components decrease in MW with increasing elution volume.

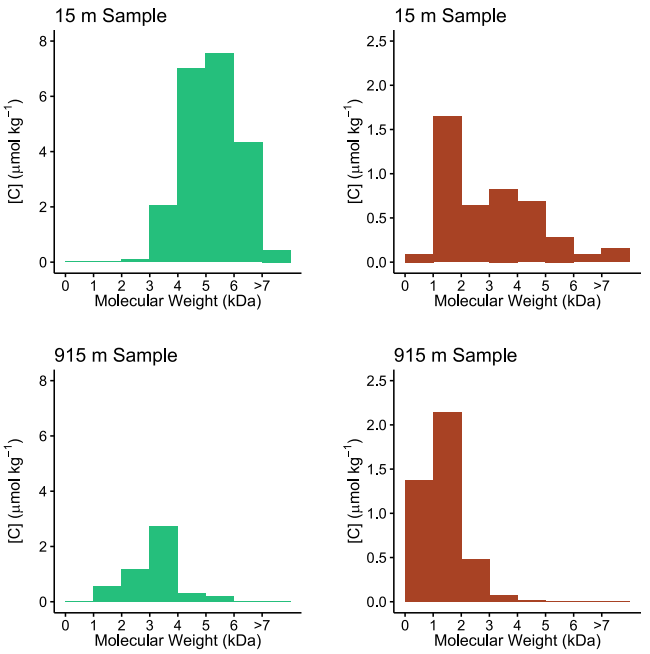

Figure 7. HMWDOM seawater concentrations (μmol C kg^{-1}) of different molecular weight classes for APS (green, left) and HS (red, right) at 15 and 915 m.

displayed a normal distribution (Shapiro-Wilk: $W = 0.85$, $p > 0.05$ for the 15 m sample and $W = 0.86$, $p > 0.05$ for the 915 m sample). At least two diagenetic pathways could explain the observed trends: A steady, continuous degradation mechanism, such as the continual hydrolysis of terminal sugars by exoenzyme activity, would result in a decrease in average MW without a change in the span of the MW distribution, as all of the polysaccharides in the APS mixture would decrease in MW at a similar rate.[30] Conversely, the decrease in MW with depth, coupled with the normal MW distribution could also be explained by the complete removal of surface-produced APS followed by replacement with APS produced at depth by autochthonous chemoautotrophy and the dissolution of sinking POC.[81] If this second mechanism is dominant, it suggests that the average MW of APS produced by these mechanisms at depth is less than the average MW of APS produced in the surface.

The minimum of APS MW plateaus at 3.5 and 2.1 kDa in the 15 and 915 m samples, respectively, well above the MWCO of the ultrafilter, suggesting there is minimal APS with a MW lower than 2.1 kDa present in seawater in the upper 1000 m of the ocean. This result raises important questions about the diagenesis of APS. Is 2.1−3.5 kDa a MW threshold below which APS is rapidly remineralized, resulting in an undetectable standing stock of APS with MW less than 2.1 kDa? While 2.1 kDa is above the 600−800 Da MW threshold for cross-membrane transport, cells may use extracellular enzymes to slowly break down APS to 2−3 kDa. At this point glycan binding proteins on the cell membrane could bind APS to the outer membrane, where further hydrolysis occurs with little to no loss of the hydrolysis products back into the environment.[31,32,82−84] To test this, chemical hydrolysis could be used to create APS with a MW less than 2.1 kDa and uptake experiments could be performed to study the lability of polysaccharides of different MWs.

HS in the 915 m sample has a narrow MW range (0.9−2.4 kDa) and displays a normal distribution (Shapiro-Wilk: $W = 0.92$, $p > 0.05$). In contrast, HS in the 15 m sample has a broad MW range (0.9−6.4 kDa) that is not normally distributed (Shapiro-Wilk: $W = 0.81$, $p < 0.05$). The broad MW distribution suggests HS in the surface ocean can be conceptualized as a mixture of higher MW HS (3.0−6.4 kDa) that is newly formed in surface waters, and a lower MW (0.9−2.4 kDa) HS component that is supplied by vertical mixing of surface and mesopelagic waters. As surface waters are transported downward by deep mixing at high latitudes, the newly formed, higher MW component of HS is degraded decreasing the span of the MW distribution. If this scenario is correct, then the radiocarbon value of surface water HS should be correlated with its MW.

The absolute abundance of HMW HS (~4 μM C) does not change significantly between the 15 and 915 m samples. This implies that HMW HS remineralization in the mesopelagic ocean may be balanced by in situ production.

Little evidence of LMWDOM fouling was found in these HMWDOM samples. Had fouling occurred, the MW of later-eluting MMC fractions would have continued to decrease below the MWCO of the filter, approaching the 300−600 Da MW of DOM isolated by SPE. Given that the MW of HS plateaued at ~900 Da, it is likely that most of the retained material should be classified as HMW. While some LMW

https://doi.org/10.1021/acs.est.4c03372
Environ. Sci. Technol. 2024, 58, 14709−14717

material may have cocollected in the UF fraction, a prior report[21] of abundant LMW HS in UF samples likely resulted from either the low sensitivity for HMW compounds exhibited by high-resolution mass spectrometers or the use of different UF membranes that experience higher degrees of fouling. It is unclear which explanation accounts for the findings of that study.

■ ASSOCIATED CONTENT

Data Availability Statement

All NMR data can be found on nmrXiv: 10.57992/nmrxiv.p65.

Supporting Information

The Supporting Information is available free of charge at https://pubs.acs.org/doi/10.1021/acs.est.4c03372.

> Full pulse sequence parameter set for the DOSY experiments; DOSY MW standard curves; validation of DOSY technique for measuring the MW of HMWDOM; and explanation of Span calculations Map of sampling location; details on the calculation of HS carbon concentration; description of DOSY validation methodology and results; experiments were run on samples under several different solvent conditions to test the effects of solute concentration, solution salinity, and solvent polarity on the measured diffusion coefficients obtained from the DOSY method; and full parameter list for the DOSY experiment (PDF)

■ AUTHOR INFORMATION

Corresponding Authors

Daniel J. Repeta − *Department of Marine Chemistry and Geochemistry, Woods Hole Oceanographic Institution, Woods Hole, Massachusetts 02543, United States*; Email: drepeta@whoi.edu

Benjamin N. Granzow − *Geoscience Research Division, Scripps Institution of Oceanography, University of California at San Diego, La Jolla, California 92093, United States; Department of Marine Chemistry and Geochemistry, Woods Hole Oceanographic Institution, Woods Hole, Massachusetts 02543, United States*; orcid.org/0000-0001-5241-4254; Email: bgranzow@ucsd.edu

Complete contact information is available at: https://pubs.acs.org/10.1021/acs.est.4c03372

Author Contributions

The manuscript was written through contributions of all authors. All authors have given approval to the final version of the manuscript.

Notes

The authors declare no competing financial interest.

■ ACKNOWLEDGMENTS

The authors thank Carl Johnson for his assistance and advice on the NMR data acquisition and Eric Grabowski and David Karl for sample elemental analysis. This work was supported by the Simons Foundation (SCOPE award 329108 and DOM^2 award 988193 to D.J.R. and Life Sciences award 990989; B.N.G.), and the Gordon and Betty Moore Foundation (6000; D.J.R.).

■ REFERENCES

(1) Verdugo, P.; Alldredge, A. L.; Azam, F.; Kirchman, D. L.; Passow, U.; Santschi, P. H. The Oceanic Gel Phase: A Bridge in the DOM-POM Continuum. *Mar. Chem.* **2004**, *92* (1−4), 67−85.

(2) Lee, C.; Wakeham, S.; Arnosti, C. Particulate Organic Matter in the Sea: The Composition Conundrum. *AMBIO: J. Hum. Environ.* **2004**, *33* (8), 565−575.

(3) Hansell, D. A.; Carlson, C. A.; Repeta, D. J.; Schlitzer, R. Dissolved Organic Matter in the Ocean: A Controversy Stimulates New Insights. *Oceanography* **2009**, *22* (4), 202−211.

(4) Cheryan, M. *Ultrafiltration Handbook*; Technomic Publishing Co. Inc.: Lancaster, PA, 1986.

(5) Roland, L. A.; McCarthy, M. D.; Peterson, T. D.; Walker, B. D. A Large-Volume Microfiltration System for Isolating Suspended Particulate Organic Matter: Fabrication and Assessment versus GFF Filters in Central North Pacific. *Limnol. Oceanogr.: Methods* **2009**, *7* (1), 64−80.

(6) Benner, R.; Pakulski, J. D.; McCarthy, M. D.; Hedges, J. I.; Hatcher, P. G. Bulk Chemical Characteristics of Dissolved Organic Matter in the Ocean. *Science* **1992**, *255* (March), 1561−1564.

(7) Guo, L.; Santschi, P. H. Ultrafiltration and Its Applications to Sampling and Characterisation of Aquatic Colloids. In *Environmental Colloids and Particles: Behavior, Separation and Characterisation*; Wilkinson, K. J.; Lead, J. R., Eds.; Wiley, 2007; Chapter 4, pp 159−221.

(8) Loh, A. N.; Bauer, J. E.; Druffel, E. R. M. Variable Ageing and Storage of Dissolved Organic Components in the Open Ocean. *Nature* **2004**, *430*, 877−881.

(9) Hansell, D. A. Recalcitrant Dissolved Organic Carbon Fractions. *Annu. Rev. Mar. Sci.* **2013**, *5*, 421−425.

(10) Walker, B. D.; Beaupré, S. R.; Guilderson, T. P.; McCarthy, M. D.; Druffel, E. R. M. Pacific Carbon Cycling Constrained by Organic Matter Size, Age and Composition Relationships. *Nat. Geosci.* **2016**, *9* (12), 888−891.

(11) Zigah, P. K.; Minor, E. C.; Abdulla, H. A. N.; Werne, J. P.; Hatcher, P. G. An Investigation of Size-Fractionated Organic Matter from Lake Superior and a Tributary Stream Using Radiocarbon, Stable Isotopes and NMR. *Geochim. Cosmochim. Acta* **2014**, *127*, 264−284.

(12) Xu, H.; Guo, L. Molecular Size-Dependent Abundance and Composition of Dissolved Organic Matter in River, Lake and Sea Waters. *Water Res.* **2017**, *117*, 115−126.

(13) Wu, F. C.; Tanoue, E.; Liu, C. Q. Fluorescence and Amino Acid Characteristics of Molecular Size Fractions of DOM in the Waters of Lake Biwa. *Biogeochemistry* **2003**, *65* (2), 245−257.

(14) Pokrovsky, O. S.; Schott, J.; Dupré, B. Trace Element Fractionation and Transport in Boreal Rivers and Soil Porewaters of Permafrost-Dominated Basaltic Terrain in Central Siberia. *Geochim. Cosmochim. Acta* **2006**, *70* (13), 3239−3260.

(15) Guo, L.; White, D. M.; Xu, C.; Santschi, P. H. Chemical and Isotopic Composition of High-Molecular-Weight Dissolved Organic Matter from the Mississippi River Plume. *Mar. Chem.* **2009**, *114* (3), 63−71.

(16) Cai, Y.; Guo, L.; Wang, X.; Aiken, G. Abundance, Stable Isotopic Composition, and Export Fluxes of DOC, POC, and DIC from the Lower Mississippi River during 2006−2008. *J. Geophys. Res.: Biogeosci.* **2015**, *120* (11), 2273−2288.

(17) Minor, E. C.; Oyler, A. R. Dissolved Organic Matter in Large Lakes: A Key but Understudied Component of the Carbon Cycle. *Biogeochemistry* **2023**, *164* (1), 295−318.

(18) Yoshioka, T.; Mostofa, K. M. G.; Konohira, E.; Tanoue, E.; Hayakawa, K.; Takahashi, M.; Ueda, S.; Katsuyama, M.; Khodzher, T.; Bashenkhaeva, N.; Korovyakova, I.; Sorokovikova, L.; Gorbunova, L. Distribution and Characteristics of Molecular Size Fractions of Freshwater-Dissolved Organic Matter in Watershed Environments: Its Implication to Degradation. *Limnology* **2007**, *8* (1), 29−44.

(19) Zigah, P. K.; Minor, E. C.; McNichol, A. P.; Xu, L.; Werne, J. P. Constraining the Sources and Cycling of Dissolved Organic Carbon in

a Large Oligotrophic Lake Using Radiocarbon Analyses. *Geochim. Cosmochim. Acta* **2017**, *208*, 102−118.
(20) Santschi, P. H.; Balnois, E.; Wilkinson, K. J.; Zhang, J.; Buffle, J.; Guo, L. Fibrillar Polysaccharides in Marine Macromolecular Organic Matter as Imaged by Atomic Force Microscopy and Transmission Electron Microscopy. *Limnol. Oceanogr.* **1998**, *43* (5), 896−908.
(21) Hertkorn, N.; Benner, R.; Frommberger, M.; Schmitt-Kopplin, P.; Witt, M.; Kaiser, K.; Kettrup, A.; Hedges, J. I. Characterization of a Major Refractory Component of Marine Dissolved Organic Matter. *Geochim. Cosmochim. Acta* **2006**, *70* (12), 2990−3010.
(22) DeFlaun, M.; Paul, J.; Jeffrey, W. Distribution and Molecular Weight of Dissolved DNA in Subtropical Estuarine and Oceanic Environments. *Mar. Ecol.: Prog. Ser.* **1987**, *38*, 65−73.
(23) Tanoue, E.; Nishiyama, S.; Kamo, M.; Tsugita, A. Bacterial Membranes: Possible Source of a Major Dissolved Protein in Seawater. *Geochim. Cosmochim. Acta* **1995**, *59* (12), 2643−2648.
(24) Powell, M. J.; Sutton, J. N.; Del Castillo, C. E.; Timperman, A. T. Marine Proteomics: Generation of Sequence Tags for Dissolved Proteins in Seawater Using Tandem Mass Spectrometry. *Mar. Chem.* **2005**, *95* (3), 183−198.
(25) Louie, S. M.; Tilton, R. D.; Lowry, G. V. Effects of Molecular Weight Distribution and Chemical Properties of Natural Organic Matter on Gold Nanoparticle Aggregation. *Environ. Sci. Technol.* **2013**, *47* (9), 4245−4254.
(26) Benner, R.; Amon, R. M. W. The Size-Reactivity Continuum of Major Bioelements in the Ocean. *Annu. Rev. Mar. Sci.* **2015**, *7* (1), 185−205.
(27) Xu, H.; Zou, L.; Guan, D.; Li, W.; Jiang, H. Molecular Weight-Dependent Spectral and Metal Binding Properties of Sediment Dissolved Organic Matter from Different Origins. *Sci. Total Environ.* **2019**, *665*, 828−835.
(28) Bartschat, B. M.; Cabaniss, S. E.; Morel, F. M. M. Oligoelectrolyte Model for Cation Binding by Humic Substances. *Environ. Sci. Technol.* **1992**, *26* (2), 284−294.
(29) Zakem, E. J.; Cael, B. B.; Levine, N. M. A Unified Theory for Organic Matter Accumulation. *Proc. Natl. Acad. Sci. U.S.A.* **2021**, *118* (6), No. e2016896118.
(30) Arnosti, C. Microbial Extracellular Enzymes and the Marine Carbon Cycle. *Annu. Rev. Mar. Sci.* **2011**, *3* (1), 401−425.
(31) Reintjes, G.; Arnosti, C.; Fuchs, B. M.; Amann, R. An Alternative Polysaccharide Uptake Mechanism of Marine Bacteria. *ISME J.* **2017**, *11* (7), 1640−1650.
(32) Cuskin, F.; Lowe, E. C.; Temple, M. J.; Zhu, Y.; Cameron, E. A.; Pudlo, N. A.; Porter, N. T.; Urs, K.; Thompson, A. J.; Cartmell, A.; Rogowski, A.; Hamilton, B. S.; Chen, R.; Tolbert, T. J.; Piens, K.; Bracke, D.; Vervecken, W.; Hakki, Z.; Speciale, G.; Munōz-Munōz, J. L.; Day, A.; Peña, M. J.; McLean, R.; Suits, M. D.; Boraston, A. B.; Atherly, T.; Ziemer, C. J.; Williams, S. J.; Davies, G. J.; Abbott, D. W.; Martens, E. C.; Gilbert, H. J. Human Gut *Bacteroidetes* Can Utilize Yeast Mannan through a Selfish Mechanism. *Nature* **2015**, *517* (7533), 165−169.
(33) Nagata, T.; Meon, B.; L Kirchman, D. Microbial Degradation of Peptidoglycan in Seawater. *Limnol. Oceanogr.* **2003**, *48* (2), 745−754.
(34) Engel, A.; Harlay, J.; Piontek, J.; Chou, L. Contribution of Combined Carbohydrates to Dissolved and Particulate Organic Carbon after the Spring Bloom in the Northern Bay of Biscay (North-Eastern Atlantic Ocean). *Cont. Shelf Res.* **2012**, *45*, 42−53.
(35) Weiss, M. S.; Abele, U.; Weckesser, J.; Welte, W.; Schiltz, E.; Schulz, G. E. Molecular Architecture and Electrostatic Properties of a Bacterial Porin. *Science* **1991**, *254* (5038), 1627−1630.
(36) Benz, R.; Bauer, K. Permeation of Hydrophilic Molecules through the Outer Membrane of Gram-Negative Bacteria. *Eur. J. Biochem.* **1988**, *176* (1), 1−19.
(37) Davidson, A. L.; Dassa, E.; Orelle, C.; Chen, J. Structure, Function, and Evolution of Bacterial ATP-Binding Cassette Systems. *Microbiol. Mol. Biol. Rev.* **2008**, *72* (2), 317−364.
(38) Alekseyeva, K. S.; Herndl, G. J.; Baltar, F. Extracellular Enzymatic Activities of Oceanic Pelagic Fungal Strains and the Influence of Temperature. *J. Fungi* **2022**, *8* (6), No. 571.
(39) Bochdansky, A. B.; Clouse, M. A.; Herndl, G. J. Eukaryotic Microbes, Principally Fungi and Labyrinthulomycetes, Dominate Biomass on Bathypelagic Marine Snow. *ISME J.* **2017**, *11* (2), 362−373.
(40) Hedges, J. I.; Cowie, G. L.; Ertel, J. R.; Barbour, R. J.; Hatcher, P. G. Degradation of Carbohydrates and Lignins in Buried Woods. *Geochim. Cosmochim. Acta* **1985**, *49* (3), 701−711.
(41) Khatami, S.; Deng, Y.; Tien, M.; Hatcher, P. G. Formation of Water-Soluble Organic Matter through Fungal Degradation of Lignin. *Org. Geochem.* **2019**, *135*, 64−70.
(42) McCarthy, M. D.; Hedges, J. I.; Benner, R. Major Biochemical Composition of Dissolved High Molecular Weight Organic Matter in Seawater. *Mar. Chem.* **1996**, *55* (3−4), 281−297.
(43) Repeta, D. J.; Quan, T. M.; Aluwihare, L. I.; Accardi, A. Chemical Characterization of High Molecular Weight Dissolved Organic Matter in Fresh and Marine Waters. *Geochim. Cosmochim. Acta* **2002**, *66* (6), 955−962.
(44) Daoud, A. B. A.; Tremblay, L. HPLC-SEC-FTIR Characterization of the Dissolved Organic Matter Produced by the Microbial Carbon Pump. *Mar. Chem.* **2019**, *215*, No. 103668.
(45) Zakem, E. J.; Levine, N. M. Systematic Variation in Marine Dissolved Organic Matter Stoichiometry and Remineralization Ratios as a Function of Lability. *Global Biogeochem. Cycles* **2019**, *33* (11), 1389−1407.
(46) Zark, M.; Dittmar, T. Universal Molecular Structures in Natural Dissolved Organic Matter. *Nat. Commun.* **2018**, *9* (1), No. 3178.
(47) Hertkorn, N.; Harir, M.; Koch, B. P.; Michalke, B.; Schmitt-Kopplin, P. High-Field NMR Spectroscopy and FTICR Mass Spectrometry: Powerful Discovery Tools for the Molecular Level Characterization of Marine Dissolved Organic Matter. *Biogeosciences* **2013**, *10*, 1583−1624.
(48) Guo, L.; Wen, L. S.; Tang, D.; Santschi, P. H. Re-Examination of Cross-Flow Ultrafiltration for Sampling Aquatic Colloids: Evidence from Molecular Probes. *Mar. Chem.* **2000**, *69* (1−2), 75−90.
(49) Ly, Q. V.; Hur, J. Further Insight into the Roles of the Chemical Composition of Dissolved Organic Matter (DOM) on Ultrafiltration Membranes as Revealed by Multiple Advanced DOM Characterization Tools. *Chemosphere* **2018**, *201*, 168−177.
(50) Pollice, A.; Brookes, A.; Jefferson, B.; Judd, S. Sub-Critical Flux Fouling in Membrane Bioreactors - a Review of Recent Literature. *Desalination* **2005**, *174* (3), 221−230.
(51) Li, K.; Huang, T.; Qu, F.; Du, X.; Ding, A.; Li, G.; Liang, H. Performance of Adsorption Pretreatment in Mitigating Humic Acid Fouling of Ultrafiltration Membrane under Environmentally Relevant Ionic Conditions. *Desalination* **2016**, *377*, 91−98.
(52) Chu, K. H.; Shankar, V.; Park, C. M.; Sohn, J.; Jang, A.; Yoon, Y. Evaluation of Fouling Mechanisms for Humic Acid Molecules in an Activated Biochar-Ultrafiltration Hybrid System. *Chem. Eng. J.* **2017**, *326*, 240−248.
(53) Šmejkalová, D.; Piccolo, A. Aggregation and Disaggregation of Humic Supramolecular Assemblies by NMR Diffusion Ordered Spectroscopy (DOSY-NMR). *Environ. Sci. Technol.* **2008**, *42* (3), 699−706.
(54) Repeta, D. J.; Aluwihare, L. I. Radiocarbon Analysis of Neutral Sugars in High-Molecular-Weight Dissolved Organic Carbon: Implications for Organic Carbon Cycling. *Limnol. Oceanogr.* **2006**, *51* (2), 1045−1053.
(55) Fourrier, P.; Dulaquais, G.; Riso, R. Influence of the Conservation Mode of Seawater for Dissolved Organic Carbon Analysis. *Mar. Environ. Res.* **2022**, *181*, No. 105754.
(56) Broek, T. A. B.; Walker, B. D.; Guilderson, T. P.; McCarthy, M. D. Coupled Ultrafiltration and Solid Phase Extraction Approach for the Targeted Study of Semi-Labile High Molecular Weight and Refractory Low Molecular Weight Dissolved Organic Matter. *Mar. Chem.* **2017**, *194*, 146−157.

https://doi.org/10.1021/acs.est.4c03372
Environ. Sci. Technol. 2024, 58, 14709−14717

(57) McCarthy, M. D.; Beaupré, S. R.; Walker, B. D.; Voparil, I.; Guilderson, T. P.; Druffel, E. R. M. Chemosynthetic Origin of ^{14}C-Depleted Dissolved Organic Matter in a Ridge-Flank Hydrothermal System. *Nat. Geosci.* **2011**, *4* (1), 32−36.
(58) De Nobili, M.; Chen, Y. Size Exclusion Chromatography of Humic Substances: Limits, Perspectives and Prospectives. *Soil Sci.* **1999**, *164* (11), 825−833.
(59) Angyal, S. J.Complexes of Metal Cations with Carbohydrates in Solution. In *Advances in Carbohydrate Chemistry and Biochemistry*; Elsevier, 1989; Vol. *47*, pp 1−43.
(60) Honda, S.; Suzuki, S.; Kakehi, K. Improved Analysis of Aldose Anomers by High-Performance Liquid Chromatography on Cation-Exchange Columns. *J. Chromatogr. A* **1984**, *291*, 317−325.
(61) Karl, D. M.; Letelier, R. M.; Bidigare, R. R.; Björkman, K. M.; Church, M. J.; Dore, J. E.; White, A. E. Seasonal-to-Decadal Scale Variability in Primary Production and Particulate Matter Export at Station ALOHA. *Prog. Oceanogr.* **2021**, *195*, No. 102563.
(62) Willcott, M. R. MestRe Nova. *J. Am. Chem. Soc.* **2009**, *131* (36), 13180.
(63) Castañar, L.; Poggetto, G. D.; Colbourne, A. A.; Morris, G. A.; Nilsson, M. The GNAT: A New Tool for Processing NMR Data. *Magn. Reson. Chem.* **2018**, *56* (6), 546−558.
(64) Beckett, R.; Jue, Z.; Giddigns, J. C. Determination of molecular weight distributions of fulvic and humic acids using flow field-flow fractionation. *Environ. Sci. Technol.* **1987**, *21*, 289−295.
(65) Reid, P. M.; Wilkinson, A. E.; Tipping, E.; Jones, M. N. Determination of Molecular Weights of Humic Substances by Analytical (UV Scanning) Ultracentrifugation. *Geochim. Cosmochim. Acta* **1990**, *54* (1), 131−138.
(66) Guéguen, C.; Cuss, C. W. Characterization of Aquatic Dissolved Organic Matter by Asymmetrical Flow Field-Flow Fractionation Coupled to UV-Visible Diode Array and Excitation Emission Matrix Fluorescence. *J. Chromatogr. A* **2011**, *1218* (27), 4188−4198.
(67) Aiken, G.; Brown, P.; Noyes, T.; Pinckney, D. Molecular Size and Weight of Fulvic and Humic Acids from the Suwannee River. In *Humic Substances in the Suwannee River, Georgia: Interactions, Properties, and Proposed Structures*; Averett, R. C.; Leenheer, J. A.; McKnight, D. M.; Thorn, K. A., Eds.; US Geological Survey Open-File Report, 1994; pp 89−99.
(68) Balch, J.; Guéguen, C. Effects of Molecular Weight on the Diffusion Coefficient of Aquatic Dissolved Organic Matter and Humic Substances. *Chemosphere* **2015**, *119*, 498−503.
(69) Aluwihare, L. I.; Repeta, D. J.; Chen, R. F. A Major Biopolymeric Component to Dissolved Organic Carbon in Surface Sea Water. *Nature* **1997**, *387* (6629), 166−169.
(70) Aluwihare, L. I.; Repeta, D. J.; Chen, R. F. Chemical Composition and Cycling of Dissolved Organic Matter in the Mid-Atlantic Bight. *Deep Sea Res., Part II* **2002**, *49* (20), 4421−4437.
(71) Johnson, C. S., Jr. Diffusion Ordered Nuclear Magnetic Resonance Spectroscopy: Principles and Applications. *Prog. Nucl. Magn. Reson. Spectrosc.* **1999**, *34*, 203−256.
(72) Carlson, D. J.; Brann, M. L.; Mague, T. H.; Mayer, L. M. Molecular Weight Distribution of Dissolved Organic Materials in Seawater Determined by Ultrafiltration: A Re-Examination. *Mar. Chem.* **1985**, *16* (2), 155−171.
(73) Guo, L.; Coleman, C. H.; Santschi, P. H. The Distribution of Colloidal and Dissolved Organic Carbon in the Gulf of Mexico. *Mar. Chem.* **1994**, *45* (1), 105−119.
(74) Guo, L.; Santschi, P. H.; Cifuentes, L. A.; Trumbore, S. E.; Southon, J. Cycling of High-Molecular-Weight Dissolved Organic Matter in the Middle Atlantic Bight as Revealed by Carbon Isotopic (^{13}C and ^{14}C) Signatures. *Limnol. Oceanogr.* **1996**, *41* (6), 1242−1252.
(75) Maurer, L. G. Organic Polymers in Seawater: Changes with Depth in the Gulf of Mexico. *Deep-Sea Res. Oceanogr. Abstr.* **1976**, *23* (11), 1059−1064.
(76) Lechtenfeld, O. J.; Kattner, G.; Flerus, R.; Mccallister, S. L.; Schmitt-Kopplin, P.; Koch, B. P. Molecular Transformation and Degradation of Refractory Dissolved Organic Matter in the Atlantic and Southern Ocean. *Geochim. Cosmochim. Acta* **2014**, *126*, 321−337.
(77) Simjouw, J.-P.; Minor, E. C.; Mopper, K. Isolation and Characterization of Estuarine Dissolved Organic Matter: Comparison of Ultrafiltration and C18 Solid-Phase Extraction Techniques. *Mar. Chem.* **2005**, *96* (3), 219−235.
(78) Reintjes, G.; Fuchs, B. M.; Amann, R.; Arnosti, C. Extensive Microbial Processing of Polysaccharides in the South Pacific Gyre via Selfish Uptake and Extracellular Hydrolysis. *Front. Microbiol.* **2020**, *11*, No. 583158.
(79) Aluwihare, L. I.; Repeta, D. J.; Pantoja, S.; Johnson, C. G. Two Chemically Distinct Pools of Organic Nitrogen Accumulate in the Ocean. *Science* **2005**, *308* (5724), 1007−1010.
(80) Quan, T. M.; Repeta, D. J. Periodate Oxidation of Marine High Molecular Weight Dissolved Organic Matter: Evidence for a Major Contribution from 6-Deoxy- and Methyl Sugars. *Mar. Chem.* **2007**, *105* (3−4), 183−193.
(81) Follett, C. L.; Repeta, D. J.; Rothman, D. H.; Xu, L.; Santinelli, C. Hidden Cycle of Dissolved Organic Carbon in the Deep Ocean. *Proc. Natl. Acad. Sci. U.S.A.* **2014**, *111* (47), 16706−16711.
(82) Arnosti, C.; Reintjes, G.; Amann, R. A Mechanistic Microbial Underpinning for the Size-Reactivity Continuum of Dissolved Organic Carbon Degradation. *Mar. Chem.* **2018**, *206*, 93−99.
(83) Martens, E. C.; Koropatkin, N. M.; Smith, T. J.; Gordon, J. I. Complex Glycan Catabolism by the Human Gut Microbiota: The Bacteroidetes Sus-like Paradigm. *J. Biol. Chem.* **2009**, *284* (37), 24673−24677.
(84) Rogowski, A.; Briggs, J. A.; Mortimer, J. C.; Tryfona, T.; Terrapon, N.; Lowe, E. C.; Baslé, A.; Morland, C.; Day, A. M.; Zheng, H.; Rogers, T. E.; Thompson, P.; Hawkins, A. R.; Yadav, M. P.; Henrissat, B.; Martens, E. C.; Dupree, P.; Gilbert, H. J.; Bolam, D. N. Glycan Complexity Dictates Microbial Resource Allocation in the Large Intestine. *Nat. Commun.* **2015**, *6* (1), No. 7481.

https://doi.org/10.1021/acs.est.4c03372
Environ. Sci. Technol. 2024, 58, 14709−14717